

RSC Advances



This is an *Accepted Manuscript*, which has been through the Royal Society of Chemistry peer review process and has been accepted for publication.

Accepted Manuscripts are published online shortly after acceptance, before technical editing, formatting and proof reading. Using this free service, authors can make their results available to the community, in citable form, before we publish the edited article. This *Accepted Manuscript* will be replaced by the edited, formatted and paginated article as soon as this is available.

You can find more information about *Accepted Manuscripts* in the [Information for Authors](#).

Please note that technical editing may introduce minor changes to the text and/or graphics, which may alter content. The journal's standard [Terms & Conditions](#) and the [Ethical guidelines](#) still apply. In no event shall the Royal Society of Chemistry be held responsible for any errors or omissions in this *Accepted Manuscript* or any consequences arising from the use of any information it contains.

ARTICLE

Silica/CdTe/Silica Fluorescent Composite Nanoparticles via Electrostatic Assembly as a pH Ratiometer

Cite this: DOI: 10.1039/x0xx00000x

Zhipeng Ran and Wuli Yang*

Received 00th January 2014,
Accepted 00th January 2014

DOI: 10.1039/x0xx00000x

www.rsc.org/

In this report, we present a ratiometric pH nanoprobe based on stable fluorescent colloidal silica composite nanoparticles encapsulating hydrophilic CdTe quantum dots. Quantum dots, owing to their fascinating optical properties, have been widely used for sensors and bioimaging. To avoid the inherent chemical instability and serious photoluminescence quenching of quantum dots, a facile electrostatic assembly method is developed to prepare sandwich-like silica/CdTe quantum dots/silica composite nanoparticles stabilized by mercaptopropyl trimethoxysilane (SQMS). This approach is of high efficiency, e.g., 98.9% of quantum dots are instantly absorbed on the surface of silica nanospheres, and nearly 80% of original fluorescence of quantum dots is retained for SQMS while traditional silica coating processes caused dramatically quenching. Finally, the bright SQMS with remarkable stability is modified with pH-sensitive fluorescein isothiocyanate to fabricate a high-resolution pH ratiometric nanoprobe. Above all, SQMS shows uniform sandwich-like structure, narrow size distribution, and stable fluorescence in strongly acidic and highly salted solutions, and the remarkable stability is in favor of quantitative analyses and nanoprobes.

1. Introduction

II–VI Semiconductor nanocrystals (or quantum dots, QDs), on account of quantum confinement effect, exhibit unique optical properties such as particle size-dependent fluorescence, broad excitation range, high quantum efficiency, and simultaneous exciting by a single light source for all colours. QDs have attracted great interest in various fields, such as nanosensors^{1–6} and theranostics.^{7, 8} However, the II–VI semiconductor nanocrystals suffer from inherent poor photoluminescence (PL) stability in harsh chemical environments, such as solutions containing plenty of metal ions or hydriions.⁹ The intrinsically unstable PL of QDs is a deadly shortcoming for their application of sensors, even though lots of ratiometric sensors have been fabricated by combining QDs with another fluorophore.^{4, 5} Since the fluorescence intensity is not specifically sensitive to a selected analyte, fluorescence fluctuation induced by multiple factors always leads to confused results in quantitative analyses. In addition, cytotoxicity caused by the release of heavy metal ions precludes the practical applications of QDs.⁹ Thus, many efforts have been dedicated to exploring suitable coating techniques to resolve the fluorescence instability and toxicity, e.g., incorporating the nanocrystals into polymer spheres^{10, 11} and silica nanoparticles^{12, 13}.

Silica nanoparticles are one of the biocompatible, inert and water dispersible materials, and a number of silica-coating procedures of QDs have undergone intensive investigations.^{14–25}

In addition to being expected to dispel the cytotoxicity as well as chemical and colloidal instability, the silica coatings ulteriorly enable surface functionalization with diverse groups. Nevertheless, the classical approaches to coat QDs with silica shell, i.e., Stöber method and reverse microemulsion approach, not only induce a dramatic decrease in QD fluorescence, but also cannot retain QD PL from harsh chemical environments.^{26, 27} To the best of our knowledge, only 57% of the initial fluorescence of CdTe QDs is retained for core/shell type of CdTe/SiO₂ nanoparticles that are prepared by reverse microemulsion method in a successful case.²⁸ Afterwards, a series of researches have focused on the silica coating methodology, such as electrostatic assembly between silica microspheres and CdSe/CdS QDs,¹⁹ and in situ growth of CdTe QDs on mercapto silica nanoparticles followed by further coating of another silica layer^{29, 30}. Although silica-coated QDs with higher relative quantum yield (QY) are acquired from these recent researches, few reports are simultaneously devoted to overcoming the fluorescence instability in harsh environments. For the significance of applications on nanosensors, it is thus highly desirable to give an in-depth and detailed illumination to preparation of silica coated QDs composites with uniform morphology, bright fluorescence, remarkable chemical stability and low cytotoxicity.

Here, we present an efficient preparation of sandwich-like silica/CdTe quantum dots/silica composite nanoparticles (SQMS) by a handy electrostatic assembly between 3-mercaptopropionic acid (MPA)-capped CdTe QDs and amino-

functionalized SiO₂ nanoparticles. The colloidal composite nearly retains 80% of initial fluorescence of CdTe QDs, and its fluorescence possesses remarkable stability in saline solution with high concentration or in buffer solution with pH values from 2 to 8. We find that the mercapto ligand exchange on the surface of QDs plays a key role in the chemical stability of fluorescence. Finally, the SQMS with remarkable stability is employed as an internal reference fluorophore and further modified with pH sensitive fluorescein isothiocyanate (FITC) to construct a pH nanoprobe (SQMSF). The QDs and FITC in SQMSF are able to be excited synchronously without dependence on fluorescence resonance energy transfer (FRET), resulting in high-resolution for the pH ratiometric sensor.

2. Experimental Section

2.1 Chemicals

Tellurium powder (98%) was acquired from Aldrich. CdCl₂ (99%), NaBH₄ (99%), and 3-mercaptopropionic acid (MPA) (99%+) were purchased from ACROS. Mercaptopropyl trimethoxysilane (MPTS), tetraethylorthosilicate (TEOS), and 3-aminopropyltriethoxysilane (APS) were obtained from Shanghai Chemical Reagents Company. Fluorescein isothiocyanate (FITC) was purchased from Beijing Huafeng United Technology Company. Ammonium hydroxide (25%~28%) was received from Taican Zhitang Chemical Co., Ltd.

2.2 Synthesis of CdTe QDs stabilized by MPA

The MPA-capped CdTe QDs were prepared according to a modified hydrothermal approach reported previously.³¹ Briefly, 100 mg of sodium borohydride (NaBH₄) was added in a flask containing 20 mL of distilled water. The flask was degassed under continuous nitrogen flow at 4 °C. Half an hour later, 127.6 mg of tellurium powder was added quickly with vigorous stirring at nitrogen atmosphere. After tellurium powder completely dissolved, purple fresh solution of sodium hydrogen telluride (NaHTe) was produced and set aside under nitrogen gas. Meanwhile, 20 mL of the solution with 20 mmol/L of CdCl₂ and 36 mmol/L of MPA was prepared. 2 mol/L of NaOH was continuously added to the solution until the pH hit 9.0. And the solution was transferred to another flask and degassed under nitrogen for 0.5 hours. 1.0 mL of as-synthesized NaHTe solution was rapidly injected into the flask with protection of nitrogen. Then, the precursor mixture was sealed into a Teflon-lined stainless steel autoclave and heated to 185 °C. After a certain time, autoclave was cooled to room temperature in cold water bath. The as-prepared CdTe QDs were precipitated by alcohol and separated by centrifugation. The time of thermal treatment would lead to different size of QDs. QD⁶⁷⁰ (top right number is the maximum emission wavelength, nm) was acquired by adjusting the reaction time to 60 min.

2.3 Synthesis of amino-functionalized silica nanoparticles (SiO₂-NH₂)

The monodispersed SiO₂-NH₂ was fabricated by a modified Stöber method.³² In detail, 15 mL ammonium hydroxide and 250 mL ethanol were mixed into a flask at 40 °C with mechanical stirring (200 rpm). 0.5 hours later, 2.5 mL of TEOS was added. And the mixture was stirred overnight continuously at 40 °C. Another 1.25 mL TEOS and 0.1 mL APS were added into flask successively with an interval of one hour. After 12 hours, the product mixture was centrifuged to collect the silica nanoparticles. The SiO₂-NH₂ was further washed with water and ethanol several times to remove the unreacted chemicals.

2.4 Synthesis of SQ, SQS and SQMS

Electrostatic self-assembly approach was explored to prepare SQMS with strong fluorescence.¹⁹ In detail, 0.5 mg of QDs was dispersed in 10 mL of deionized water (DI water). 30 mg of SiO₂-NH₂ and 0.5 mL of phosphate buffer solution (PBS, pH=5.5) were added to the QDs suspension successively. Several minutes later, the QDs would be electrostatically absorbed on the surface of SiO₂-NH₂ to form silica/CdTe quantum dots (SQ) and the SQ was separated by centrifugation and washed with water and ethanol for further use. And the supernate was collected to determine amount of unassembled QDs. The Stöber method was utilized again to coat the SQ with another outer layer of silica. In a typical procedure, the SQ was dispersed in 10 mL of ethanol with 0.5 mL of ammonium hydroxide. After 2 μL MPTS and 50 μL TEOS were added in succession, the mixture was vigorously stirred at room temperature for 6 hours. The silica/CdTe quantum dots/silica composite nanoparticles (SQMS) were centrifuged from suspension and purified by washing with water and ethanol. Compared with SQMS, SQS were also prepared at the absence of MPTS.

2.5 Synthesis of SQMSF

The mixture of 6 μL APS and 2 mg FITC was dissolved in 2 mL ethanol, and stirred for 12 hours to form FITC-APS conjugation. Here, the excess APS was used and the FITC-APS conjugation was not isolated and directly used in the next step. The as-prepared SQMS was redispersed in a flask containing 10 mL ethanol and 0.5 mL ammonium hydroxide. For modification of FITC, 40 μL FITC-APS was added in the flask simultaneously and stirred for 4 hours continuously. The products were separated and purified by centrifugation and marked as SQMSF.

2.6 Characterization

Hydrodynamic size distribution and zeta potential of particles were measured by Malvern Zetasizer Nano. Fluorescent spectra were collected by FLS920 at 25 °C. The UV-vis absorption was measured on Lambda 35. JEM-2100F field emission transmission electron microscope (FETEM) was used to analyse the size and morphology.

2.6.1 Determination of relative PL QY of SQMS to QDs

Almost all QDs were anchored on the surface of SiO₂-NH₂, which indicated nearly 100 % of electrostatic self-assembly yield. So, the PL spectra were measured at equivalent QDs concentration for QDs or SQMS to determine relative PL QY of SQMS to QDs.

2.6.2 Measurement of PL stability at different pH

QDs or SQMS with equivalent QD concentration was dispersed in a series of citric acid/disodium hydrogen phosphate buffer solution (CPBS) with various pH values from 8 to 3. Hydrochloric acid was used to further decrease the pH value to 1. After 0.5 hour, PL spectra were collected. To measure time-resolved PL stability of SQMS, the equal samples were dispersed into CPBS at pH 4.1 with a certain period of time interval. All samples were measured at the same time.

2.6.3 Determination of reversibility

The SQMSF was kept in DI water. A certain volume of SQMSF dispersion was taken out and dispersed into CPBS with pH values of 8 or 4 to determine the initial value of fluorescent intensity ratio. Then, the SQMSF was centrifuged from suspension and redispersed into CPBS with pH value of 8.1. After 10 min, the SQMSF was re-centrifuged and transferred to CPBS at pH 4.1. During each step, aliquots of SQMSF were

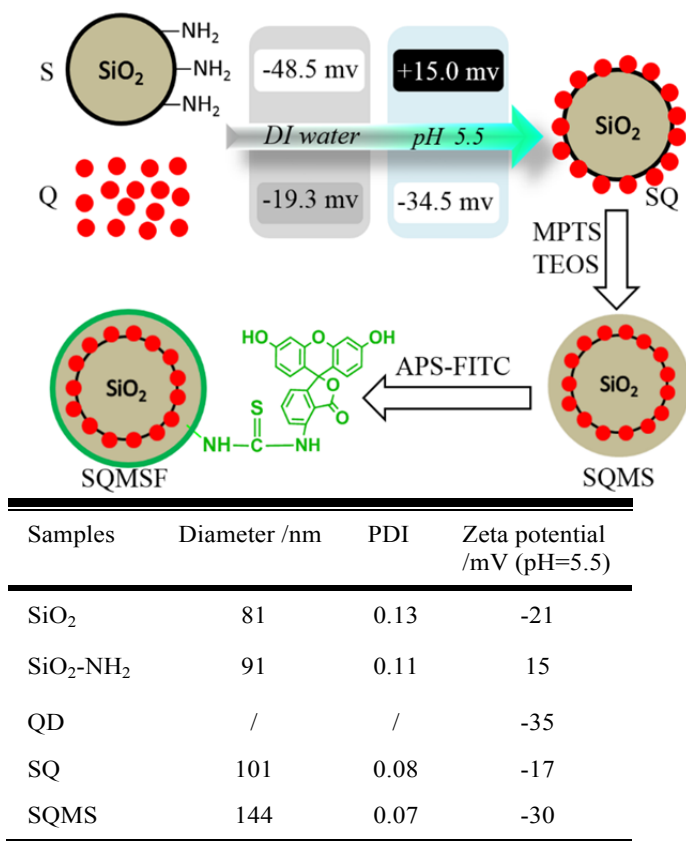
withdrawn for PL measurement. Two cycles were processed to determine the reversibility and stability.

3. Result and discussion

3.1 Synthesis of SQMS

Indeed, silica coatings of QDs have been studied extensively.³³⁻³⁵ Thereinto, a large proportion of the researches are based on Stöber method and reverse microemulsion approach. Both methods, however, suffer from a dramatic decrease in the fluorescence. Regardless of the mechanism of PL quenching, the compromise on fluorescence hampers further applications of these colloidal nanoparticles. Moreover, the silica shell seems deficient to overcome the fluorescent instability of QDs.^{16, 20, 36}

potentials. As presented in Table 1, we monitor zeta-potential of samples in following steps. QDs are dispersed in DI water in a beaker, and a suspension of SiO₂-NH₂ nanoparticles is dropped into the QD dispersion. The pH value of the mixture is adjusted to 5.5 with PBS, inducing zeta potential of SiO₂-NH₂ dramatically changing to +15 mV with a reversal from negative to positive charge, while zeta potential of QDs drops to -35 mV on the sharp contrary. The QDs are assembled on the surface of SiO₂-NH₂ completely and immediately to form SQ by strong binding interaction between the surface amino groups of SiO₂-NH₂ and QDs^{37, 38}. Owing to the anchor of QDs on SiO₂-NH₂, the zeta potential of SQ drops to -17 mV at pH 5.5. To increase their fluorescence and colloidal stability, another silica layer is then coated onto the surface of SQ via Stöber method. The further decrease of zeta potential of SQMS indicates that the SQ is completely coated by the outer silica layer.



Scheme 1. Electrostatic assembly of amino-functionalized silica nanoparticles (SiO₂-NH₂) and MPA-capped CdTe quantum dots, and preparation of pH ratiometer.

Table 1. Size distribution and zeta potential of samples.

Here, to avoid the huge drop of QD PL during encapsulating QDs within silica shells, a facile electrostatic assembly approach is developed to prepare sandwich-like silica nanoparticles with a middle layer of QDs.¹⁹ As briefly outlined in Scheme 1, first we prepare monodispersed silica nanoparticles with amino groups on the surface. The existence of amino group is verified by zeta-potential. The zeta potential of SiO₂-NH₂ is higher than SiO₂, implying that SiO₂-NH₂ is successfully amino-functionalized (Table 1). The electrostatic interactions between particles greatly depend on their zeta

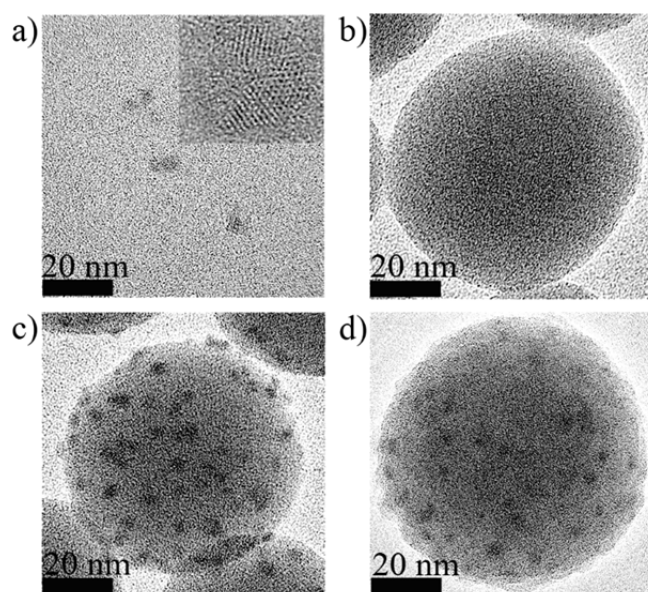


Fig. 1 TEM images for a) CdTe QDs, b) SiO₂-NH₂, c) SQ and d) SQMS.

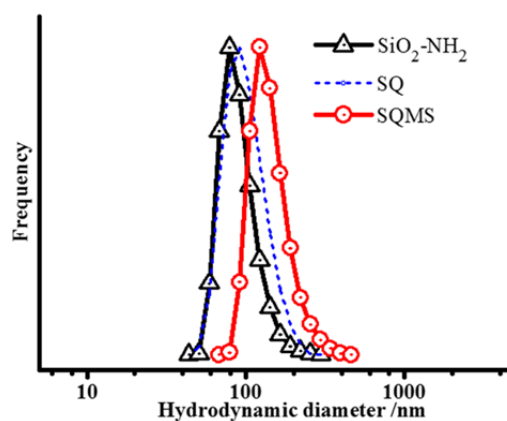


Fig. 2 Size distribution of SiO₂-NH₂, SQ and SQS acquired from DLS

Fig. 1 shows the morphology and structure for QDs, SiO₂-NH₂, SQ and SQMS observed in detail by high-resolution TEM. Lower magnification images with more particles and size information are presented in supporting information (Fig. S1). The QD crystals with the maximum emission peak of 670 nm are about 5 nm in diameter. SiO₂-NH₂ shows uniform spheres

with flat surface and average size of 65 ± 5 nm in diameter. Fig. 1c shows clearly that some black dots on the surface of $\text{SiO}_2\text{-NH}_2$ for SQ and no obvious aggregation of QDs is observed. The average size of SQMS becomes slightly larger and increases to 71 ± 7 nm, another silica layer about 3 nm is coated on SQ. The hydrodynamic diameter of samples is also investigated by dynamic light scattering (DLS) to estimate size distribution as shown in Fig. 2. The hydrodynamic size is 101 nm for SQ, slightly larger than 91 nm of $\text{SiO}_2\text{-NH}_2$, and increases to 144 nm for SQMS after coated with the outer silica layer. All of $\text{SiO}_2\text{-NH}_2$, SQ and SQMS nanospheres present narrow size distribution with a polydispersity index of 0.11, 0.08 and 0.07 respectively.

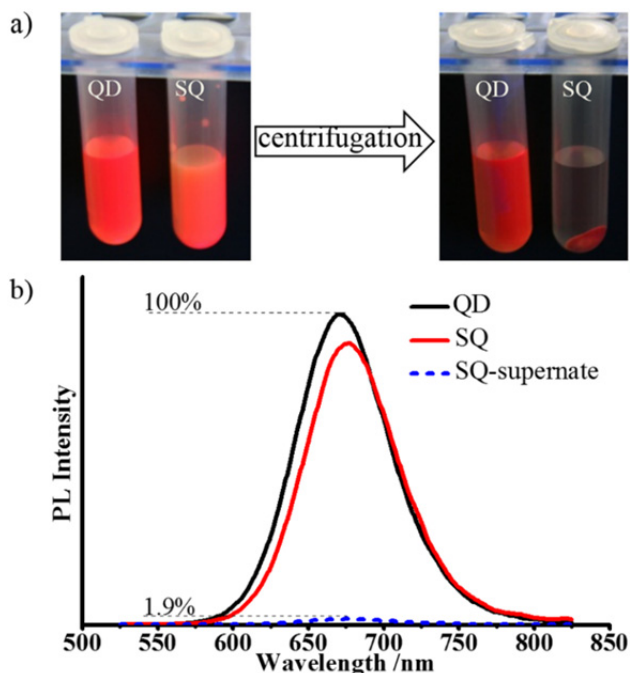


Fig. 3 a) Water dispersion of QD and SQ excited under a 365 nm ultraviolet (UV) lamp. b) Quantitative analysis by fluorescent spectra.

Then fluorescent methodology is employed to calculate the loading efficiency of QDs. After addition of PBS (pH 5.5) to aqueous dispersion of QDs and $\text{SiO}_2\text{-NH}_2$, QDs are immediately absorbed on the surface of $\text{SiO}_2\text{-NH}_2$. Considering QDs are very stable in aqueous dispersion and not able to be precipitated by centrifugation as results of smaller size and stabilization of MPA, we centrifuge the mixture to separate SQ and collect the supernate that contains unloaded QDs (Fig. 3a). Under irradiation of an ultraviolet lamp, the QDs dispersion and SQ precipitate show bright red fluorescence while nearly no emission from supernate is observed by naked eye. The result manifests almost all of QDs are loaded onto SQ. And a dramatic increase of absorption for SQ also indicates the incorporation of QDs (Fig. S2). Further quantitative analysis by fluorescent spectra indicates that about 98.9% of QDs are loaded to SQ and the assembly process has little effect on QY of QDs (Fig. 3b). These findings strongly demonstrate that the current electrostatic assembly is more rapid to fabricate composite silica nanoparticles encapsulating QDs with uniform sandwich-like structure and high loading efficiency.

3.2 Fluorescence and stability of SQMS.

Stability of QDs fluorescence is of particular importance, and the goal of the silica coating is to improve the chemical stability of QDs and retain fairly considerable fluorescence at the same time. QDs should be at least stable between pH 4 and pH 8 when used for biology, since pH values in human body fall in this range.²⁷ For broader applications, especially as fluorescent probes, the chemical instability of QDs remains a problem. The PL stability of QDs is surveyed in buffer solution and NaCl solution (Fig. S3, S4 and S5).²⁰ As Fig. 4b and 4c show, PL of pure QDs is completely quenched at pH 4.0 or 200 mM NaCl solution. Even in NaCl solution at concentration of 150 mM corresponding with ionic strength in human body, the fluorescence of QDs is seriously quenched and only about 10% of initial fluorescence is retained. These conspicuous fluorescence instabilities under different environments seriously hamper QD applications in quantitative imaging. In the most successful solution, stable QDs have been acquired by combining the silica and amphiphilic polymer encapsulation techniques, but huge drop of fluorescence still exists.²⁷

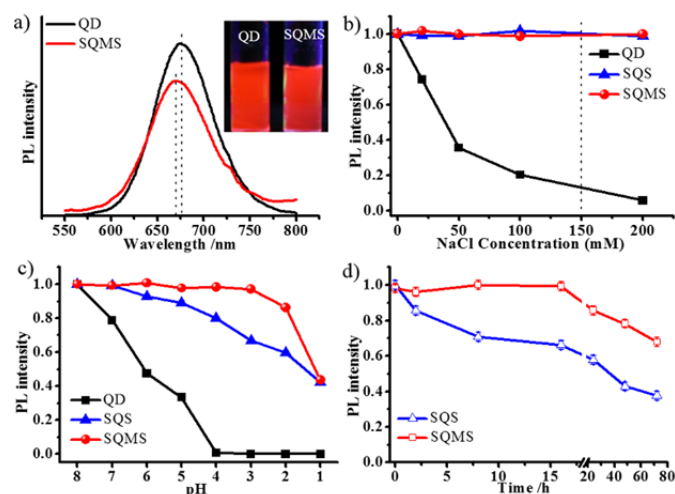


Fig. 4 a) Fluorescent spectra of QD and SQMS dispersions with equivalent QD concentration. Inset: a digital photo of QD and SQMS excited under a 365 UV lamp. b) The influence of ionic strength on PL emission. The dash line indicates the ionic strength in human body. c) PL intensity of samples in buffer solution at pH values from 1 to 8. d) Stability of PL intensity versus time for SQS and SQMS in buffer solution at pH 4.

In this work, we present a simple silica coating approach with ligand exchange. After encapsulated in silica, nearly 80% of the original fluorescence is preserved for SQMS, and aqueous dispersion of SQMS shows bright red fluorescence, almost commensurate with pure QDs (Fig. 4a). The considerable fluorescence retention can be attributed to pre-anchoring of QDs on the surface of $\text{SiO}_2\text{-NH}_2$ before the following silica coating via Stöber method. And the ligand exchange from MPA to MPTS induces blue shift of about 5 nm for maximum emission as described elsewhere (Fig. 4a).²⁹

The ligand exchange is in favor of the stability of SQMS. After coated with silica shell, the PL of SQS and SQMS becomes inert for NaCl at concentration below 200 mM, indicating the silica shell plays a key role in PL stability. However, H^+ still slightly quenches the PL of SQS. On one hand the carboxyl group of MPA ligand on QDs has significant effect on pH sensitivity of PL.⁹ On the other hand due to pore-structure and hydrophilic essence of silica nanoparticles prepared by Stöber method or reverse microemulsion method,

silica coating is not enough to protect QDs from permeation of hydrogen ions.^{20, 26} So MPTS is employed to stabilize the SQ in coating process. SQMS shows remarkable stability to H⁺ at pH values between 2 to 8, even no fluorescence quenching appears in buffer solution at pH 4 within 16 hours (Fig. 4d), and indicating the ligand exchange between MPTS and MPA facilitates the improvement of PL stability. The bright fluorescence and remarkable stability of SQMS are of great benefit to biology use, such as imaging and biosensors.

3.2 pH ratiometric sensor

Finally, we show that the SQMS with stable fluorescence can be used to configurate a pH probe.³⁹ Since the fluorescence of QDs are often sensitive to H⁺, diverse metal ions¹, proteins³³, etc., they have been widely used to probe pH values in biomedical researches through the change of their fluorescence emission intensity.⁴⁰ However, the intensity of excitation light, absolute concentration of QDs, and loss due to photobleaching also have significant effect on fluorescence intensity, resulting in that the single QDs sensors are of little use. Therefore numerous recent works have built QD-based ratiometric sensors by combining QDs with another fluorophore.^{5, 41} These internal reference/sensitivity dual emissive pairs rather than single QDs generate fluorescence intensity ratios irrespective of factors aforementioned. And it will be better if the reference fluorophore and sensor dye are able to be excited at the same time by a monochromatic light rather than excited respectively. To this end, pH ratiometric sensors based on FRET have been intriguing considerable interests.^{4, 5} However, owing to the essence of FRET, the PL peaks of reference and sensor dye are too close to be distinguished for the sensor. Besides, fluorescence of QDs is not specifically sensitive to pH values. Credible result is elicited from neither single QDs probes nor QDs based ratiometric sensors because the presence of other ions could also change the fluorescence intensity of QDs. Thus, instability of QDs should be eliminated before using QDs as pH sensors as well as other probes.

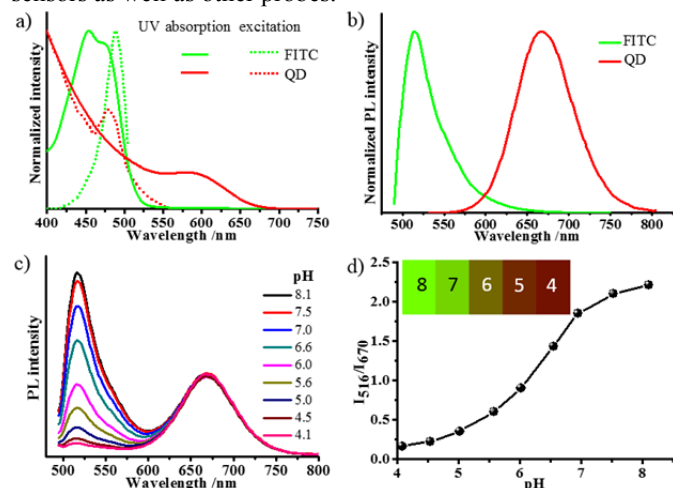


Fig. 5 a) UV-vis and excitation spectra for FITC and QDs. b) PL spectra for FITC and QDs. c) PL spectra of SQMSF at various pH values, excited at 488 nm. d) Working curve of FITC/QD⁶⁷⁰ fluorescence intensity ratios (I_{516}/I_{670}) versus pH values. Insert: pseudofluorescent images of SQMSF aqueous solution at pH values from 8 to 4.

Here, to construct a high resolution pH ratiometer, stable SQMS with the maximum emission of 670 nm is used as an internal reference and further modified with pH-sensitive FITC

with maximum emission of 516 nm. Due to the effective overlap of absorption spectra for QDs and FITC, they are able to be synchronously excited by a monochromatic light of 488 nm without the assistance of FRET (Fig. 5a), which is also proved by the fluorescence lifetime measurements (Fig. S6). And the size-dependent tuneable emission for QDs endows QD/FITC pairs with high distinguishability for their PL peaks (Fig. 5b). As pH increases from 4.1 to 8.1, the PL intensity ratio of FITC to QDs (I_{516}/I_{670}) rises from 0.2 to 2.1 (Fig. 5d). The dependence of I_{516}/I_{670} versus pH values is similar to that of FITC with pK_a of about 6.4⁵ (Fig. S7), while PL of QDs keeps constant at pH values from 4.1 to 8.1 (Fig 4c). There is almost no overlap for PL peaks of FITC (516 nm) and QDs (670 nm) excited by a monochromatic light of 488 nm simultaneously (Fig. 5c), indicating high resolution of SQMSF for pH. In the stability test, I_{516}/I_{670} has little change at pH 8.1 or 4.1 for SQMSF kept in water, indicating SQMSF has remarkable stability and reversibility in water (Fig. 6, red circle and green triangle). However, one must notice that slight leakage of FITC in alkaline aqueous solution cannot be avoided due to cleavage of Si-O-Si induced by self-catalysis of amine groups of APS (Scheme S2).^{42, 43}

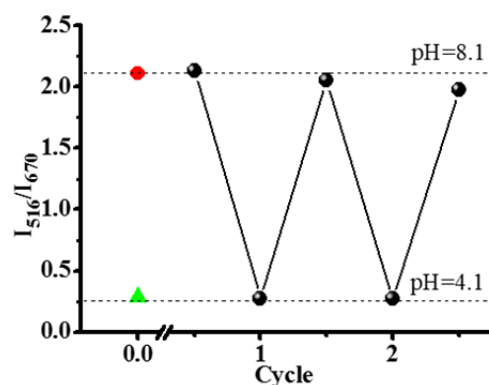


Fig. 6 Reversibility and stability of SQMSF. The red circle and green triangle represent I_{516}/I_{670} of original SQMSF for pH 8.1 and 4.1 respectively. The SQMSF is kept in water before reversibility test.

Conclusions

In conclusion, highly fluorescent and stable sandwich-like SQMS is prepared by a simple and efficient electrostatic self-assembly approach. Nearly 98.9% of QDs are loaded onto composite nanoparticles. SQMS is 71 ± 7 nm in diameter, retaining 80% of initial fluorescence, with uniform morphology and robust stability in NaCl solution and at pH values from 4 to 8 due to the ligand exchange from MPA to MPTS. Then SQMS is modified with FITC for the application as a pH ratiometric sensor. Owing to tuneable PL and large Stokes shift for QDs, the SQMSF is able to be simultaneously excited by a monochromatic light and shows high resolution in PL peaks. I_{516}/I_{670} changes from 0.2 to 2.1 as pH values increasing from 4 to 8, indicating SQMSF can be used to determine H⁺ accurately.

Acknowledgements

We acknowledge the support from the National Science Foundation of China (Grant No. 51273047) and the ‘‘Shu Guang’’ Project (12SG07) supported by Shanghai Municipal Education Commission and Shanghai Education Development Foundation.

Notes and references

* State Key Laboratory of Molecular Engineering of Polymers and Department of Macromolecular Science, Fudan University, Shanghai 200433, China; Fax: +86 21-6564 0293; Tel: +86 21-6564 2385; E-mail: wlyang@fudan.edu.cn.

† Electronic Supplementary Information (ESI) available. See DOI:10.1039/b000000x/

1. P. Wu, T. Zhao, S. Wang and X. Hou, *Nanoscale*, 2014, **6**, 43.
2. B. J. Kim, K. Paek, H. Yang, J. Lee and J.W. Park, *ACS Nano*, 2014, **8**, 2848
3. Q. Ma, Y. Li, Z. H. Lin, G. C. Tang and X. G. Su, *Nanoscale*, 2013, **5**, 9726.
4. P. T. Snee, R. C. Somers, G. Nair, J. P. Zimmer, M. G. Bawendi and D. G. Nocera, *J. Am. Chem. Soc.*, 2006, **128**, 13320.
5. T. Jin, A. Sasaki, M. Kinjo and J. Miyazaki, *Chem Commun*, 2010, **46**, 2408.
6. S. Huang, F. Zhu, H. Qiu, Q. Xiao, Q. Zhou, W. Su and B. Hu, *Colloids and Surfaces B: Biointerfaces*, 2014, **117**, 240.
7. Y. P. Ho and K. W. Leong, *Nanoscale*, 2010, **2**, 60.
8. X. Michalet, F. F. Pinaud, L. A. Bentolila, J. M. Tsay, S. Doose, J. J. Li, G. Sundaresan, A. M. Wu, S. S. Gambhir and S. Weiss, *Science*, 2005, **307**, 538.
9. Y. Li, L. Jing, R. Qiao and M. Gao, *Chem Commun*, 2011, **47**, 9293.
10. Y. Yang, Z. Wen, Y. Dong and M. Gao, *Small*, 2006, **2**, 898.
11. N. Tomczak, R. R. Liu and J. G. Vancso, *Nanoscale*, 2013, **5**, 12018.
12. T. Nann and P. Mulvaney, *Angew. Chem. Int. Ed.*, 2004, **43**, 5393.
13. L. Jing, C. Yang, R. Qiao, M. Niu, M. Du, D. Wang and M. Gao, *Chem. Mater.*, 2009, **22**, 420.
14. Z. Lin, X. Fei, Q. Ma, X. Gao and X. Su, *N. J. Chem.*, 2014, **38**, 90.
15. G. Stoica, I. C. Serrano, A. Figuerola, I. Ugarte, R. Pacios and E. Palomares, *Nanoscale*, 2012, **4**, 5409.
16. Y. Zhang, M. Wang, Y. G. Zheng, H. Tan, B. Y. W. Hsu, Z. C. Yang, S. Y. Wong, A. Y. C. Chang, M. Choolani, X. Li and J. Wang, *Chem. Mater.*, 2013, **25**, 2976.
17. C. L. Li and N. Murase, *J. Colloid Interface Sci.*, 2013, **411**, 82.
18. W. S. Song, J. H. Kim and H. Yang, *Mater. Lett.*, 2013, **111**, 104.
19. M. Cho, K. Lim and K. Woo, *Chem Commun*, 2010, **46**, 5584.
20. C. Wang, Q. Ma, W. Dou, S. Kanwal, G. Wang, P. Yuan and X. Su, *Talanta*, 2009, **77**, 1358.
21. S. Wang, C. Li, P. Yang, M. Ando and N. Murase, *Colloids and Surfaces A: Phys. Eng. Aspects*, 2012, **395**, 24.
22. K. Han, Z. Xiang, Z. Zhao, C. Wang, M. Li, H. Zhang, X. Yan, J. Zhang and B. Yang, *Colloids and Surfaces A: Phys. Eng. Aspects*, 2006, **280**, 169.
23. B. H. Jun, D. W. Hwang, H. S. Jung, J. Jang, H. Kim, H. Kang, T. Kang, S. Kyeong, H. Lee, D. H. Jeong, K. W. Kang, H. Youn, D. S. Lee and Y.-S. Lee, *Adv. Funct. Mater.*, 2012, **22**, 1843.
24. C. Wu, J. Zheng, C. Huang, J. Lai, S. Li, C. Chen and Y. Zhao, *Angew. Chem. Int. Ed.*, 2007, **46**, 5393.
25. M. F. Foda, L. Huang, F. Shao and H. Y. Han, *ACS Applied Mater. & Interfaces*, 2014, **6**, 2011.
26. M. Szekeres, J. Toth and I. Dekany, *Langmuir*, 2002, **18**, 2678.
27. X. G. Hu and X. H. Gao, *ACS Nano*, 2010, **4**, 6080.
28. L. Jing, C. Yang, R. Qiao, M. Niu, M. Du, D. Wang and M. Gao, *Chem. Mater.*, 2010, **22**, 420.
29. Y. Zhu, Z. Li, M. Chen, H. M. Cooper, G. Q. Lu and Z. P. Xu, *Chem. Mater.*, 2012, **24**, 421.
30. Y. Zhu, Z. Li, M. Chen, H. M. Cooper and Z. P. Xu, *J. Mater. Chem. B*, 2013, **1**, 2315.
31. J. Guo, W. Yang and C. Wang, *J. Mater. Chem. B*, 2005, **109**, 17467.
32. Z. Ran, Y. Sun, B. Chang, Q. Ren and W. Yang, *J. Colloid Interface Sci.*, 2013, **410**, 94.
33. R. Koole, M. M. van Schooneveld, J. Hilhorst, C. de Mello Donegá, D. C. Hart, A. van Blaaderen, D. Vanmaekelbergh and A. Meijerink, *Chem. Mater.*, 2008, **20**, 2503.
34. M. Darbandi, R. Thomann and T. Nann, *Chem Mater.*, 2005, **17**, 5720.
35. Q. Ma, I. C. Serrano and E. Palomares, *Chem Commun*, 2011, **47**, 7071.
36. P. Yang, N. Murase and J. Yu, *Colloids and Surfaces A: Phys. Eng. Aspects*, 2011, **385**, 159.
37. C. Graf, S. Dembski, A. Hofmann and E. Ruhl, *Langmuir*, 2006, **22**, 5604.
38. N. Liu, B. S. Prall and V. I. Klimov, *J. Am. Chem. Soc.*, 2006, **128**, 15362.
39. M. F. Frasco and N. Chaniotakis, *Sensors*, 2009, **9**, 7266.
40. I. L. Medintz, M. H. Stewart, S. A. Trammell, K. Susumu, J. B. Delehanty, B. C. Mei, J. S. Melinger, J. B. Blanco-Canosa, P. E. Dawson and H. Mattoussi, *Nature Mater.*, 2010, **9**, 676.
41. M. Amelia, A. Lavie-Cambot, N. D. McClenaghan and A. Credi, *Chem Commun*, 2011, **47**, 325.
42. M. Etienne, *Talanta*, 2003, **59**, 1173.
43. O. Seitz, P. G. Fernandes, R. Tian, N. Karnik, H.-C. Wen, H. Stiegler, R. A. Chapman, E. M. Vogel and Y. J. Chabal, *J. Mater. Chem.*, 2011, **21**, 4384.